

Cuk Converter Fed Adjustable Speed DC Motor Driven Electrical Single Stage Centrifugal Pump

SASWATI SWAPNA DASH¹, BYAMAKESH NAYAK²

¹Department of Electrical Engineering, ²School of Electrical Engineering
YMCA University of science and technology¹, KIIT University²

¹Faridabad, Haryana, ²Bhubaneswar, Odisha

INDIA

reachtoswapna@gmail.com¹, electricbkn@gmail.com²

Abstract: - This paper presents a Robust Control of Cuk Converter Fed DC motor drive connected to an electrical single stage centrifugal Pump for small scale irrigation. Cuk converter can be used for both voltage buck and boost mode with polarity reversal. In this paper the transient modeling of Cuk converter with motor load and electrical single stage centrifugal pump is carried out. The averaging is done by state-space average analysis followed by small signal model analysis for linearization. The compensators for closed loop control are designed by classical control technique. The experiment is done in MATLAB work environment and the result is verified by Simulation.

Key-Words: - Cuk converter, Current mode control, separately excited DC motor, state-space average analysis, electrical single stage (ESS) centrifugal pump, small signal analysis, robust control, small scale irrigation.

1 Introduction

Power electronics plays an important role in adjustable DC motor drive system. The efficiency, reliability and power regulation of DC motor drive increases by using different dc-dc converters. Due to the fast development and better switching control of static switches these drives are applied for various applications. The basic necessity is irrigation of water to the fields for proper production of crops to meet the demand. In the remote areas where no ac supply is given till date and the necessity of small scale irrigation is required, in such places these battery supplied DC motor driven centrifugal pumps can be used for the same. Afterward the battery can be replaced by or connected to any renewable source like solar, wind or hybrid to have a constant source of power in remote areas with better control [1]. Advantages over direct converters, the indirect DC-DC converters have wide application with higher range of speed control. Both isolating and non-isolating indirect dc-dc converters are now applied for most latest DC motor with centrifugal pump system for better performance. Among these the boost-buck converter also known as cuk converter has unique identification due to its different configuration of circuit using a capacitor as main storage device with polarity reversal possibilities [2]. The basic block diagram of a feed back control system of a Cuk converter with separately excited DC motor load along with an electrical single stage centrifugal pump is shown in

Fig.1. Transient modeling analysis is done by state-space averaging method followed by small signal model analysis. The compensators for the speed loop and the current loop are designed based on the frequency responses as well as root locus technique for the system [3]-[5]. An electrical single stage centrifugal pump is chosen for the operation in small scale irrigation [6], [7]. A robust control technique is used for improving transient response and tested in Matlab/Simulink environment.

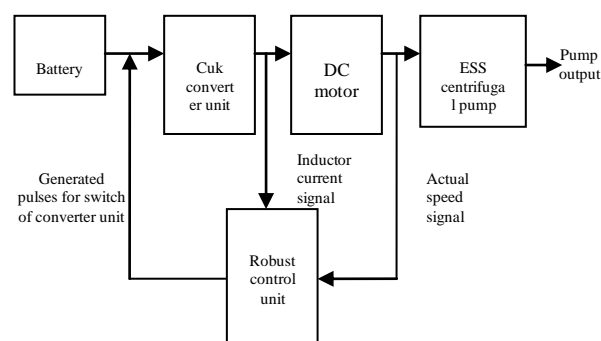


Fig. 1. Block diagram of Cuk converter controlled separately excited dc motor drive with an electrical single stage centrifugal pump.

2 State-Space Average Analysis Of Cuk Converter With Motor Load And Electrical Single Stage Centrifugal Pump

The transient modeling and analysis of Cuk converter with motor load along with an electrical single stage centrifugal pump can be explained in two modes. Assuming continuous conduction mode, there are two modes one is called duty interval mode, where capacitor voltage appear across the load by turning on the switch and other is freewheeling mode where diode is on to short the armature terminals of motor [8]-[13]. Five state variables are needed to represent the state-space averaged model of proposed system. The simple separately excited DC motor is used in this investigation [14]-[16]. The load torque here is the mechanical torque (T_1) of the pump, which is directly proportional to the ‘head’ of the pump and here it is considered as a non-linear function of the

motor speed i.e. $K_1 \omega_m^2$, where $K_1 = 9.6 \times 10^{-4}$. The Kirchoff’s Voltage Law, Kirchoff’s Current Law expression in terms of the inductor current and capacitor voltage when switch is on are (the equations are formed by assuming Cuk converter exhibits a polarity reversal between input and output) given as follows:

$$L_1 \frac{di_{11}}{dt} = V_{in} \tag{1}$$

$$L_2 \frac{di_{12}}{dt} + R_a i_{12} + K_b \omega_m - v_c = 0 \tag{2}$$

$$C \frac{dv_c}{dt} = -i_{12} \tag{3}$$

Where $L_1, i_{11}, V_{in}, L_2, i_{12}, R_a, K_b, \omega_m, v_c, C$ are inductance 1 in henry, input current in ampere, input voltage in volt, inductance 2 in henry, armature current in ampere, armature resistance in ohm, back emf constant in N-m/amp, angular speed in rad/sec, capacitor voltage in volt and capacitance in mF respectively.

Now the fundamental torque equation for the motor-load system is given by (4),

$$T_e - T_1 = \frac{j(d\omega_m)}{dt} + B\omega_m \tag{4}$$

The above equation can be written as:

$$\left. \begin{aligned} j \frac{d\omega_m}{dt} &= K_b i_{12} - B\omega_m - T_1 \\ T_e &= K_b i_{12} \end{aligned} \right\} \tag{5}$$

Since,

$$T_1 = K_1 \omega_m^2 \quad (\text{For centrifugal pump})$$

Now putting all the values in (4), and differentiating both sides,

$$j\dot{a} + Ba + 2K_1 \omega_m a = K_b \frac{di_1}{dt} \tag{6}$$

Where,

$$\frac{d\omega_m}{dt} = a \tag{7}$$

$$\frac{da}{dt} = \frac{K_b v_c}{L_2 j} - \frac{K_b^2 \omega_m}{L_2 j} - \frac{K_b R_a i_{12}}{L_2 j} - \frac{a(B+2K_1 \omega_m)}{j} \tag{8}$$

Where j, T_e, T_1, B, a represent moment of inertia of motor in kg-m^2 , instantaneous torque in N-m, load torque in N-m, viscous friction in N-m-s/rad and rate of change of speed respectively. The (1), (2), (3), (5), (7) and (8) can be represented in state-space form as follows:

$$\begin{bmatrix} \frac{di_{11}}{dt} \\ \frac{di_{12}}{dt} \\ \frac{dv_c}{dt} \\ \frac{d\omega_m}{dt} \\ \frac{da}{dt} \end{bmatrix} = \begin{bmatrix} 0 & 0 & 0 & 0 & 0 \\ 0 & -\frac{R_a}{L_2} & \frac{1}{L_2} & -\frac{K_b}{L_2} & 0 \\ 0 & -\frac{1}{C} & 0 & 0 & 0 \\ 0 & 0 & 0 & 0 & 1 \\ 0 & -\frac{K_b R_a}{L_2 j} & \frac{K_b}{L_2 j} & -\frac{K_b^2}{L_2 j} & -\frac{(B+2K_1 \omega_m)}{j} \end{bmatrix} \begin{bmatrix} i_{11} \\ i_{12} \\ v_c \\ \omega_m \\ a \end{bmatrix} + \begin{bmatrix} V_{in} \\ L_1 \\ 0 \\ 0 \\ 0 \\ 0 \end{bmatrix} \tag{8}$$

$$A_1 = \begin{bmatrix} 0 & 0 & 0 & 0 & 0 \\ 0 & -\frac{R_a}{L_2} & \frac{1}{L_2} & -\frac{K_b}{L_2} & 0 \\ 0 & -\frac{1}{C} & 0 & 0 & 0 \\ 0 & 0 & 0 & 0 & 1 \\ 0 & -\frac{K_b R_a}{L_2 j} & \frac{K_b}{L_2 j} & -\frac{K_b^2}{L_2 j} & -\frac{(B+2K_1 \omega_m)}{j} \end{bmatrix}$$

Where

$$B_1 U_1 = \begin{bmatrix} V_{in} \\ L_1 \\ 0 \\ 0 \\ 0 \\ 0 \end{bmatrix}$$

and

Similarly when switch is off, the diode is on. Based on KCL and KVL the equations can be

written as follows:

$$L_2 \frac{di_{12}}{dt} + R_a i_{12} + K_b \omega_m = 0 \quad (9)$$

$$L_1 \frac{di_{11}}{dt} + v_c = V_{in} \quad (10)$$

$$C \frac{dv_c}{dt} = i_{11} \quad (11)$$

$$\frac{d\omega_m}{dt} = a \quad (12)$$

$$\frac{da}{dt} = \frac{K_b v_c}{L_2 j} - \frac{K_b R_a}{L_2 j} i_{12} - \frac{K_b^2 \omega_m}{L_2 j} - \frac{a(B+2K_1 \omega_m)}{j} \quad (13)$$

The state-space form of above equations (9) to (13) can be represented as follows:

$$\begin{bmatrix} \frac{di_{11}}{dt} \\ \frac{di_{12}}{dt} \\ \frac{dv_c}{dt} \\ \frac{d\omega_m}{dt} \\ \frac{da}{dt} \end{bmatrix} = \begin{bmatrix} 0 & 0 & -\frac{1}{L_1} & 0 & 0 \\ 0 & -\frac{R_a}{L_2} & 0 & -\frac{K_b}{L_2} & 0 \\ \frac{1}{C} & 0 & 0 & 0 & 0 \\ 0 & 0 & 0 & 0 & 1 \\ 0 & -\frac{K_b R_a}{L_2 j} & 0 & -\frac{K_b^2}{L_2 j} & -\frac{(B+2K_1 \omega_m)}{j} \end{bmatrix} \begin{bmatrix} i_{11} \\ i_{12} \\ v_c \\ \omega_m \\ a \end{bmatrix} + \begin{bmatrix} V_{in} \\ L_1 \\ 0 \\ 0 \\ 0 \end{bmatrix} \quad (14)$$

Where

$$A_2 = \begin{bmatrix} 0 & 0 & -\frac{1}{L_1} & 0 & 0 \\ 0 & -\frac{R_a}{L_2} & 0 & -\frac{K_b}{L_2} & 0 \\ \frac{1}{C} & 0 & 0 & 0 & 0 \\ 0 & 0 & 0 & 0 & 1 \\ 0 & -\frac{K_b R_a}{L_2 j} & 0 & -\frac{K_b^2}{L_2 j} & -\frac{(B+2K_1 \omega_m)}{j} \end{bmatrix}$$

$$B_2 U_2 = \begin{bmatrix} V_{in} \\ L_1 \\ 0 \\ 0 \\ 0 \end{bmatrix} \quad (15)$$

and Let the switching function of self commutated controlled switch and diode is q_1 and q_2 respectively. Assuming the continuous conduction mode, the averaged model is obtained by

substituting d for q_1 and $1-d$ for q_2 . The state-space average model is represented as:

$$\dot{X} = AX + BU$$

$$Y = CX$$

$$\text{Where } A = dA_1 + (1-d)A_2$$

$$\text{and } BU = dB_1 U_1 + (1-d)B_2 U_2 \quad (16)$$

Substituting (7) and (13) in (14) results,

$$A = \begin{bmatrix} 0 & 0 & -\frac{(1-d)}{L_1} & 0 & 0 \\ 0 & -\frac{R_a}{L_2} & \frac{d}{L_2} & -\frac{K_b}{L_2} & 0 \\ \frac{(1-d)}{C} & -\frac{d}{C} & 0 & 0 & 0 \\ 0 & 0 & 0 & 0 & 1 \\ 0 & -\frac{K_b R_a}{L_2 j} & \frac{dK_b}{L_2 j} & -\frac{K_b^2}{L_2 j} & -\frac{(B+2K_1 \omega_m)}{j} \end{bmatrix}$$

$$BU = \begin{bmatrix} V_{in} \\ L_1 \\ 0 \\ 0 \\ 0 \end{bmatrix} \quad (17)$$

Hence the state-space average form can be derived as follows:

$$\begin{bmatrix} \frac{di_{11}}{dt} \\ \frac{di_{12}}{dt} \\ \frac{dv_c}{dt} \\ \frac{d\omega_m}{dt} \\ \frac{da}{dt} \end{bmatrix} = \begin{bmatrix} 0 & 0 & -\frac{(1-d)}{L_1} & 0 & 0 \\ 0 & -\frac{R_a}{L_2} & \frac{d}{L_2} & -\frac{K_b}{L_2} & 0 \\ \frac{(1-d)}{C} & -\frac{d}{C} & 0 & 0 & 0 \\ 0 & 0 & 0 & 0 & 1 \\ 0 & -\frac{K_b R_a}{L_2 j} & \frac{dK_b}{L_2 j} & -\frac{K_b^2}{L_2 j} & -\frac{(B+2K_1 \omega_m)}{j} \end{bmatrix} \begin{bmatrix} i_{11} \\ i_{12} \\ v_c \\ \omega_m \\ a \end{bmatrix} + \begin{bmatrix} V_{in} \\ L_1 \\ 0 \\ 0 \\ 0 \end{bmatrix} \quad (18)$$

3 Modelling of Centrifugal Pump

The affinity law is used to draw the performance curve of head and flow rate at the nominal speed.

The flow rate Q is directly proportional to impeller speed and the head (H) is directly proportional to

square of speed ω_m . Since the hydraulic power (P) is directly proportional to the head and flow rate therefore it is proportional to the cube of speed

(ω^3).i.e. $K_1\omega_m^3$.this law is applicable only above the

threshold speed (ω_s).For less than the threshold value the pressure produced by the pump is less than the static pressure and the rotation just circulate water within the pump [17]. The characteristic of centrifugal pump with valve completely opened is illustrated in Fig.2 and the speed Vs centrifugal load torque graph is shown in Fig. 3.

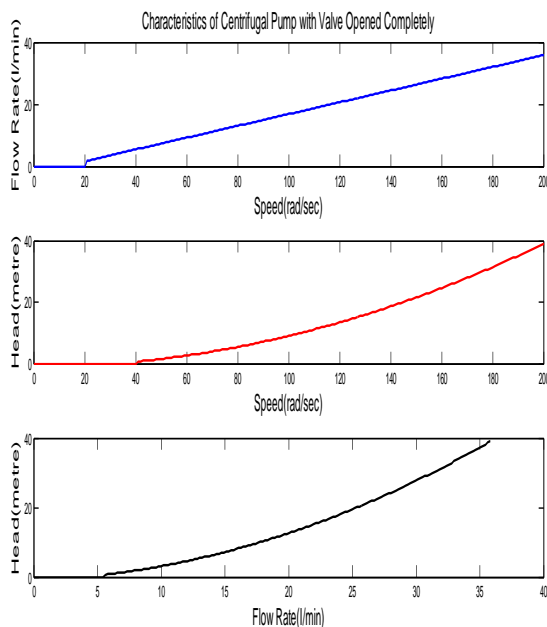


Fig.2. Characteristics of centrifugal pump with valve completely opened.

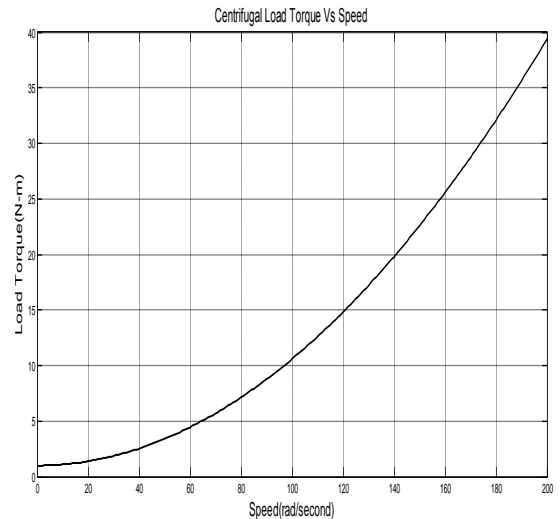


Fig. 3 Speed (ω_s) Vs Centrifugal Load Torque (T_1)

$$Q = a\omega - b \text{ (Where } \omega \geq \text{Threshold speed } (\omega_s)) \tag{19}$$

$$Q = 0 \text{ (When } \omega \leq \text{Threshold speed } (\omega_s)) \tag{20}$$

The value of ‘a’ and ‘b’ depend upon the static head and decreases with the increase of the pumping head and it has maximum value when the discharge valve is fully opened [1].

The head equation can be written as

$$H = c\omega^2 - d\omega \tag{21}$$

Where the values of ‘c’ and ‘d’ depend on the valve setting. Since the hydraulic power is proportional to the head flow rate product. It is represented as:

$$R_h = c_1\omega^3 - c_2\omega^2 + c_3\omega \tag{22}$$

The Torque developed by the motor depends upon the head and therefore it is directly proportional to the square of the speed. To start the centrifugal pump, a breakaway torque of above 10-20% of nominal torque is required to overcome the static friction of the moving part involved. For variable head drive system, the speed of the motor is required to be controlled. In this paper, the speed is regulated depending on the head of the system.

This electrical single stage centrifugal pump is a kind of volute pumps. In general the energy calculated is:

$$E = \frac{V_w H}{267} \tag{23}$$

Where, E =Energy in kilowatt hour or watt hour

V_w =Volume of water in m^3 , H =Head in metres

Again power calculated is:

$$P = \frac{E}{T} \tag{24}$$

$$P = 9.81QH \tag{25}$$

Where, P =Power in watt, T =Time in hour

Q =Discharge in litres per second

The Cuk DC-DC converter is in between the battery and DC motor, used here to control the speed of the motor by controlling the armature voltage below and above the input battery voltage. Changing speed of the motor keeping flow rate constant is proposed in this paper.

4 Small-Signal Analysis

The state-space averaged model of Cuk converter with active machine load shown in (18) is

non linear in nature as the control parameter \hat{d} is in

matrix A . Therefore small-signal analysis is required to make the state-space to be linear [18]. Due to

small variation of \hat{d} in steady state D the state

variables are changed to $i_{L1} + \hat{i}_{L1}$, $i_{L2} + \hat{i}_{L2}$, $V_c + \hat{v}_c$

and $\omega_m + \hat{\omega}_m$. Assuming constant load torque and

without disturbance in input voltage the state-space averaged model (18) with small perturbation is modified by (26),

$$\begin{bmatrix} \frac{d(i_{L1} + \hat{i}_{L1})}{dt} \\ \frac{d(i_{L2} + \hat{i}_{L2})}{dt} \\ \frac{d(V_c + \hat{v}_c)}{dt} \\ \frac{d(\omega_m + \hat{\omega}_m)}{dt} \\ \frac{d(a + \hat{a})}{dt} \end{bmatrix} = \begin{bmatrix} 0 & 0 & -\frac{(1-D-\hat{d})}{L_1} & 0 & 0 \\ 0 & -\frac{R_a}{L_2} & \frac{D+\hat{d}}{L_2} & -\frac{K_b}{L_2} & 0 \\ (1-D-\hat{d}) & -\frac{D+\hat{d}}{C} & 0 & 0 & 0 \\ 0 & 0 & 0 & 0 & 1 \\ 0 & -\frac{K_b R_a}{L_2 j} & \frac{(D+\hat{d})K_b}{L_2 j} & -\frac{K_b^2}{L_2 j} & -\frac{(B+2K_1 \omega_m)}{j} \end{bmatrix} \begin{bmatrix} i_{L1} + \hat{i}_{L1} \\ i_{L2} + \hat{i}_{L2} \\ V_c + \hat{v}_c \\ \omega_m + \hat{\omega}_m \\ a + \hat{a} \end{bmatrix} + \begin{bmatrix} \frac{V_{in}}{L_1} \\ 0 \\ 0 \\ 0 \\ 0 \end{bmatrix} \tag{26}$$

Subtracting (18) from (26) and neglecting higher order perturbation terms, the small-signal model of Cuk converter without any mechanical load torque can be written as:

$$\begin{bmatrix} \frac{d\hat{i}_{L1}}{dt} \\ \frac{d\hat{i}_{L2}}{dt} \\ \frac{d\hat{v}_c}{dt} \\ \frac{d\hat{\omega}_m}{dt} \\ \frac{d\hat{a}}{dt} \end{bmatrix} = \begin{bmatrix} 0 & 0 & -\frac{(1-D)}{L_1} & 0 & 0 \\ 0 & -\frac{R_a}{L_2} & \frac{D}{L_2} & -\frac{K_b}{L_2} & 0 \\ (1-D) & -\frac{D}{C} & 0 & 0 & 0 \\ 0 & 0 & 0 & 0 & 1 \\ 0 & -\frac{K_b R_a}{L_2 j} & \frac{DK_b}{L_2 j} & -\frac{K_b^2}{L_2 j} & -\frac{(B+2K_1 \omega_m)}{j} \end{bmatrix} \begin{bmatrix} \hat{i}_{L1} \\ \hat{i}_{L2} \\ \hat{v}_c \\ \hat{\omega}_m \\ \hat{a} \end{bmatrix} + \begin{bmatrix} \frac{V_c}{L_1} \\ \frac{V_c}{L_2} \\ -\frac{(i_{L1} + i_{L2})}{C} \\ 0 \\ \frac{K_b V_c}{L_2 j} \end{bmatrix} [\hat{d}] \tag{27}$$

The small signal step responses and bode diagrams are shown for inductor current, armature current, capacitor voltage, speed and rate of change of speed are represented in following fig.4 and fig.5 respectively. These figures are describing the effect of system parameters on the stability of the system. The bode diagrams briefly explain the phase margin and gain margin of the system. Here the noise will pass to the output. Hence the closed loop control will take care of noise by designing appropriate filter in feedback loop. The overshoot and settling time is always desired less for a better system. So for that all the design parameters are properly calculated. In closed loop control the proper design of feedback loop will eliminate most of the undesired elements of the existing system. Bode plot of inductor current has a gain margin of infinity and phase margin of 89.8748, where the phase cross over frequency is 711.12.

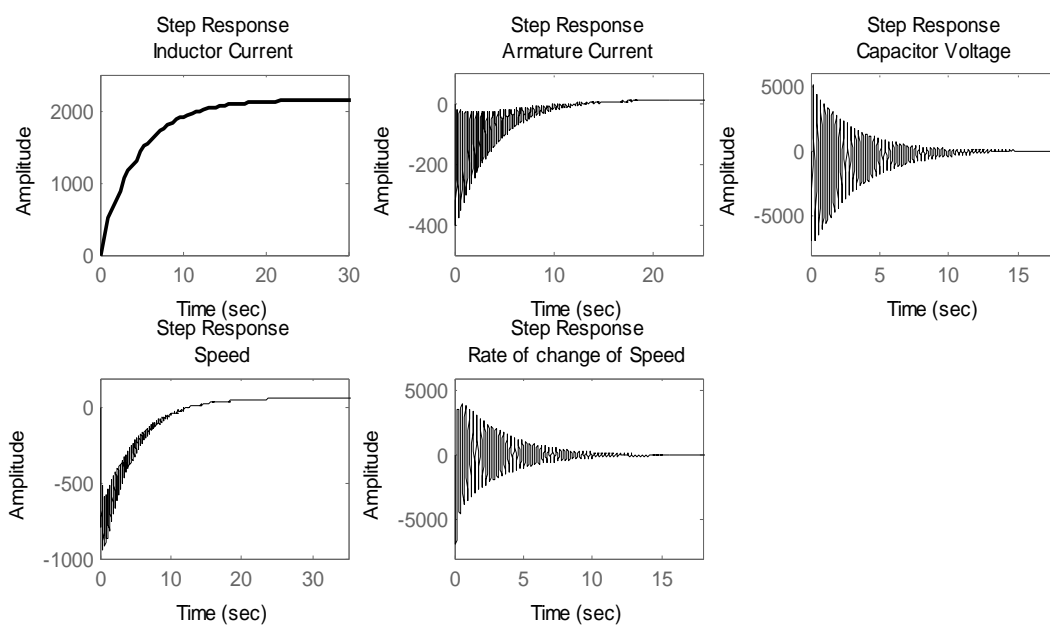


Fig.4. Small signal step responses for Inductor current, Armature current, Capacitor voltage, Speed and Rate of change of speed.

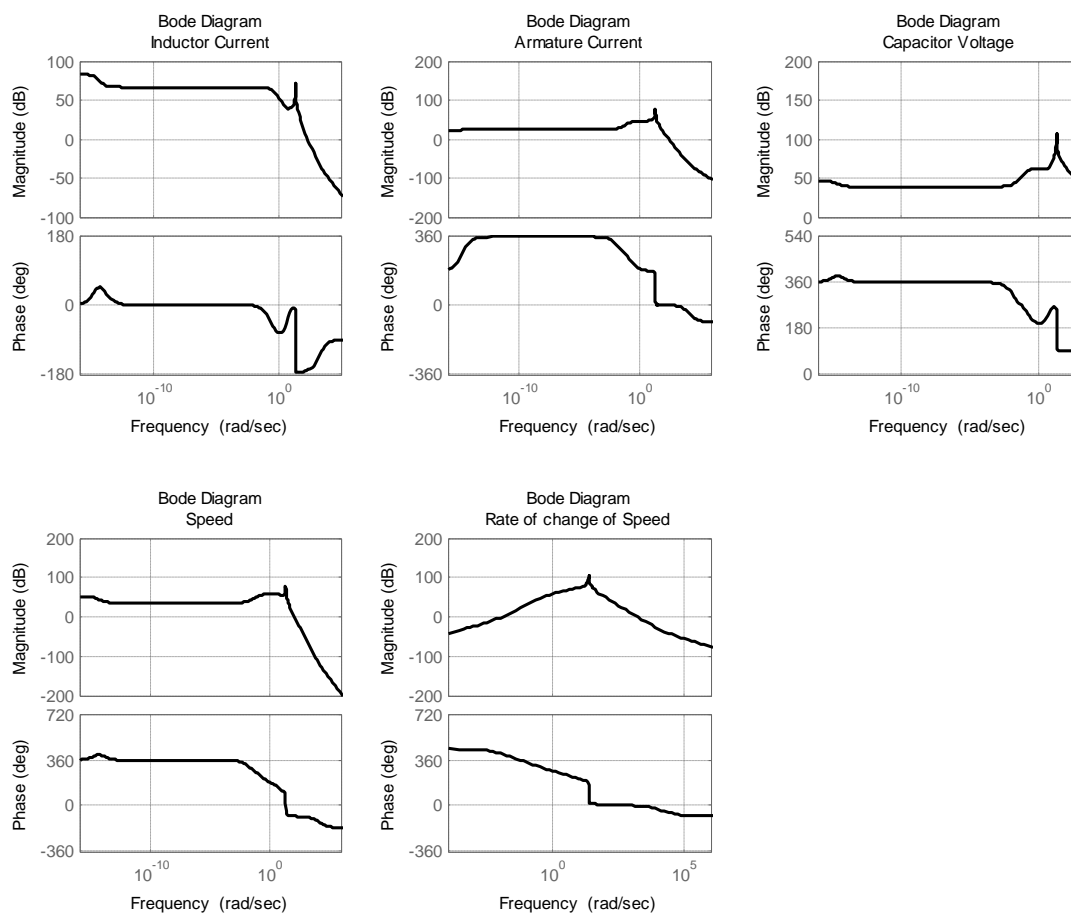


Fig.5. Small signal bode diagrams for Inductor current, Armature current, Capacitor voltage, Speed and Rate of change of speed.

5 Steady-State Analysis and Transfer Function

The steady-state equations can be derived from averaged state-space model (16) and represented as:

$$V_c = \frac{V_{in} D}{1-D} \tag{28}$$

$$\frac{i_{L1}}{i_{L2}} = \frac{D}{1-D} \tag{29}$$

$$\frac{K_b \omega_m + R_a i_{L2}}{V_{in}} = \frac{D}{1-D} \tag{30}$$

$$T_L = K_b i_{L2} - B \omega_m \tag{31}$$

The Boost-Buck converter exhibits the reversal polarity between input and output voltage

since $\frac{D}{1-D} > 0$ at any value of D (equations are derived based on reverse polarity of output voltage). Fig. 6 shows the relationship between the modulus of voltage gain and duty cycle. The small signal model parameters in Table-1 are derived from a practical system and Fig.7 demonstrate the simulated response during step change of duty ratio D from 0.8 to 0.9.

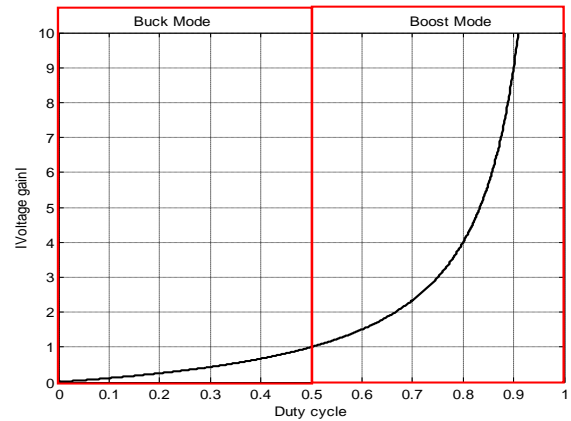


Fig. 6. Modulus of voltage gain versus duty cycle of Cuk converter controlled separately excited dcmotor drive.

TABLE I
Small Signal Model Parameters

V_i	48V
R_a	0.5Ω
L_1	0.27H
L_2	1.326H
C	1.31mF
D	0.8
B	0.02N-m-s/rad
J	0.05Kg-m ²
f_s	10kHz
K_b	1.23N-m/amp
T_l	0 N-m

Simulated responses during step change of Duty ratio (D) from 0.8 to 0.9

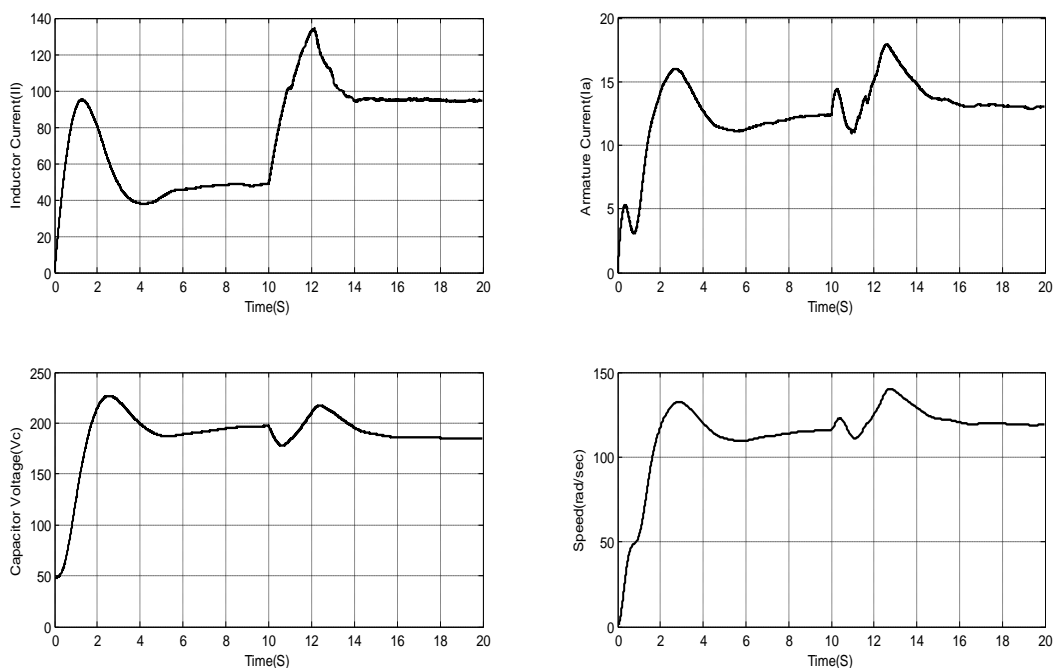


Fig.7. Simulated response during step change of duty ratio D from 0.8 to 0.9.

6 Current Mode Control of Cuk Converter

The derived transfer functions from small-signal model can be used for current mode control method. In current mode control method there are two loops one is inner input current loop and other is outer speed loop where actual speed follow the reference speed. In inner loop, the direct measurement of input current is compared with the reference input current estimated from the speed

loop. The error is compensated using $G_{ci}(S)$. Hence the loop transfer function of inner current loop is

$G_{ci}(S) * G_{i1d}(S)$. The switching function $\hat{d}(t)$ is

determined from the output of $G_{ci}(S)$ through hysteresis band controller. In outer speed loop, the direct measurement of actual speed is compared with reference speed. The error is compensated

using $G_{cw}(S)$. The output of $G_{cw}(S)$ is the reference input current command which is processed by actual current by inner loop. The block diagram of current control mode is shown in Fig. 8.

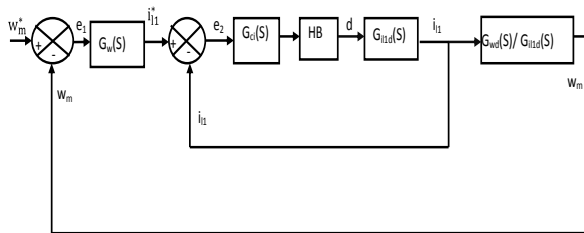


Fig.8. Block diagram of closed loop speed control of separately excited dc motor drive.

Here the outer loop is highly coupled with inner loop because of input current command is generated from outer loop which is the command value of inner loop. The coupling behavior can be represented by,

$$(i_{11}^* - i_{11})G_{ci}(S) = \hat{d} \tag{32}$$

Substituting the value of i_{11} by,

$$i_{11}^* G_{ci}(S) = \hat{d}(1 + G_{i1d}(S) G_{ci}(S)) \tag{33}$$

Now the input current command-to-speed transfer function is given by,

$$G_{wil1}(s) = \frac{\hat{\omega}_m(s)}{i_{11}^*(s)} = \frac{G_{wd}(S)G_{ci}(S)}{(1+G_{i1d}(S)G_{ci}(S))} \tag{34}$$

7 Simulation Results

In order to keep the flow rate constant for different head, the speed control of DC motor with centrifugal pump is required. The actual speed of the motor is compared with the command speed estimated from the head and the error is processed through a compensator. The output of the compensator is the inductor current command. In the current mode control method, the inner loop, where the direct measurement of inductor current is compared with the reference inductor current. The output is fed to hysteresis band modulator and the pulses are generated for the switches of Cuk converter. The compensator is designed based upon frequency responses.

The compensator for speed loop is designed using classical control technique and root locus method. Step responses of 80 rad/s for 20 seconds and at 20 seconds step response command increased to 120 rad/s are used to observe the dynamic characteristics of inductor current, armature current, capacitor voltage speed respectively. The inductor current, armature current and capacitor voltage and speed responses of change of step reference from 80rad/s to120rad/s is shown in Fig. 9, Fig. 10 , Fig. 11 , Fig. 12 respectively. It has been observed that both of the speed responses reach the respective steady state value without exhibiting the oscillation. The settling time for high speed response is lower than the low speed step response command. Settling time for 80rad/s is 12 seconds and for 120rad/s is about 9 seconds.

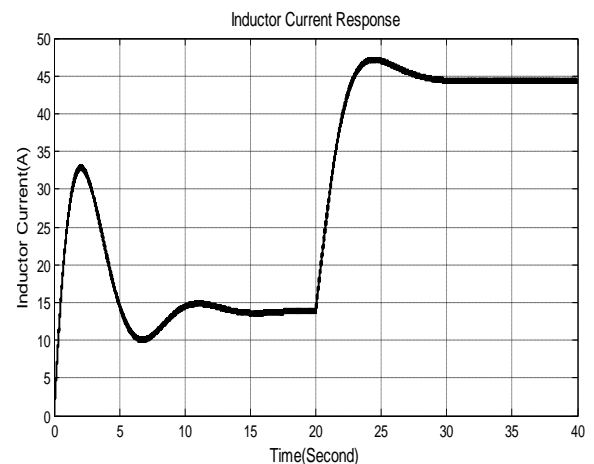


Fig.9. Inductor Current Response of closed loop Cuk converter control of DC motor with ESS centrifugal pump for a change of step response from 80 rad/s to 120 rad/s.

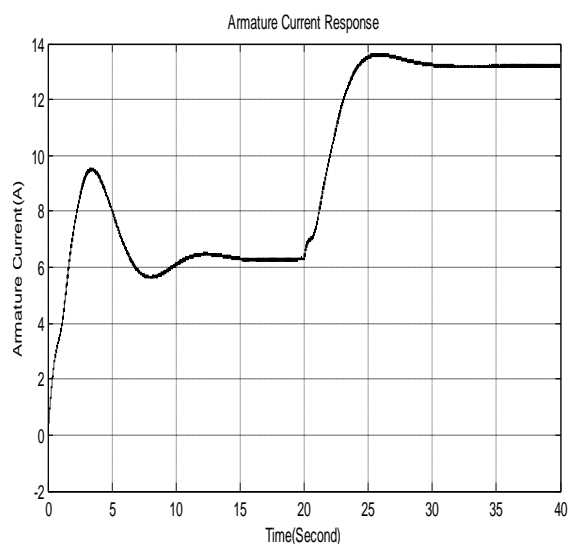


Fig.10. Armature Current Response of closed loop Cuk converter control of DC motor with ESS centrifugal pump for a change of step response from 80 rad/s to 120 rad/s.

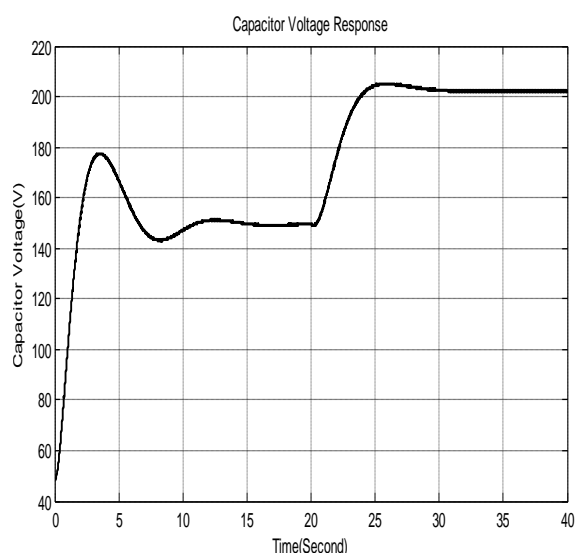


Fig.11. Capacitor Voltage Response of closed loop Cuk converter control of DC motor with ESS centrifugal pump for a change of step response from 80 rad/s to 120 rad/s.

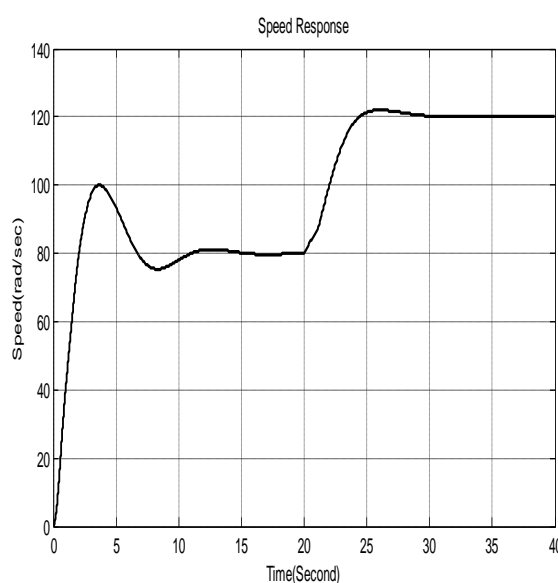


Fig.12. Speed Response of closed loop Cuk converter control of DC motor with ESS centrifugal pump for a change of step response from 80 rad/s to 120 rad/s.

8 Conclusion

This paper presents detailed transient analysis of Cuk converter used for speed control of DC motor with ESS centrifugal pump. The further analysis is done using small-signal analysis for linearization. Hysteresis band controller is used here which is a kind of robust control. The simulation results reveal that, the over shoot and settling time of compensated system is less compared to the uncompensated system. Advance controller can be employed for better switching performance and hence better result and can promote small scale irrigation in agriculture sector.

Appendix

Machine rating and parameters: 5HP, 240V separately excited with $R_a=0.5\text{ohm}$, $L_a=0.01\text{H}$, $K_b=1.23\text{N-m/Amp}$, $R_f=240\text{ohm}$, $J=0.05\text{Kg-m}^2$, $B=0.02\text{N-m-s/rad}$ and No load speed= 193.8rad/s .

References:

- [1] M.A.Elegandy, B.Zahawi, and D.J. Atkinson, "Comparison of directly connected and constant voltage controlled photovoltaic pumping systems," *IEEE Transactions in sustainable energy*, Vol.1, 2010, pp.184-192 Oct.
- [2] P.Krein, *Elements of Power Electronics*, New York: Oxford University Press, 1998.
- [3] K.Smedley, and S.Cuk, "Switching flow graph nonlinear modelling technique," *IEEE Transactions in Power Electronics*, Vol.9,

- Jul.1994, pp.405-413.
- [4] Billy B.Y.Lau, "Small-signal frequency response theory for ideal DC-DC converter systems," Ph.D. Thesis, California institute of Technology, June 1986.
- [5] B.K.Nayak, Saswati Swapna Dash, "Battery Operated Closed Loop Speed Control of DC Separately Excited Motor by Boost-Buck Converter", *IEEE International conference on power electronics (IICPE-2012)*, Dec., 2012.
- [6] R.Andoulssi,A.Draou,H.Jerbi,A.Alghonamy,B. Khiari, "Non linear control of a photo voltaic pumping system, " *Energy Procedia 42(2013),Elsevier*, 2013, pp.328-336.
- [7] Saswati Swapna Dash, B.K.Nayak, Subrat Kumar, "Feedback Control and Dynamic Behaviour of Z-source Converter Fed Separately Excited DC Motor and Centrifugal pump set," *International Journal of Engineering and Technology*, Vol.6, no.3, ,Jun-July 2014, pp.1601-1613.
- [8] R.D.Middlebrook and S.Cuk, "A general unified approach to modelling switching converter power stages," in *Proc.1976 IEEE PESC*, pp.18-34.
- [9] Poh.ChiangLoh, D.M.Vilathgamuwa, C.J.Gajanayake and C.W.Teo, "Transient Modelling and Analysis of Pulse-width modulated Z-Source Inverter," *IEEE Transactions in Power Electronics*, Vol.22, March.2007, pp.498-507.
- [10] R.Krishnan, *Electric motor drives modeling, analysis and control*, Pearson education pvt.ltd. 2003.
- [11] L.Umanand, *Power electronic essentials and applications*, Vol. I. New York: Wiley publishers, 2009.
- [12] P.C.Loh, P.C.Tan, F.Blaabjerg, and T.K.Lee, "Topological development and operational analysis of Buck-Boost current source inverter for energy conversion applications," in *Proc. 2006 IEEE PESC*, pp.1-6.
- [13] G.F.Franklin, J.D.Powel and A.Emami-Naeini, *Feedback Control of Dynamic Systems, 3rd ed. Reading, MA: Addison-Wesley*, 1994.
- [14] Oshaba, A.S., Ali, E.S., "Bacteria foraging: A new technique for speed control of DC series motor supplied by photovoltaic system", *WSEAS Transactions on Power Systems*, Vol. 9, 2014, Pages 185-195.
- [15] Oshaba, A.S., Ali, E.S., "Swarming speed control for DC permanent magnet motor drive via pulse width modulation technique and DC/DC converter", *Research Journal of Applied Sciences, Engineering and Technology*, Vol. 5, No. 18, 2013, Pages 4576-4583.
- [16] S. M. Abd-Elazim, and E. S. Ali, "Synergy of Particle Swarm Optimization and Bacterial Foraging for TCSC Damping Controller Design", *WSEAS Transactions on Power Systems*, Vol. 8, No. 2, April 2013, pp. 74-84.
- [17] Seleshi Bekele Awulachew (IWMI),Philippe Lemperiere (IWMI),Taffa Tulu (Adama University), "pumps for small scale irrigation, " *Module 4-Improving Productivity and Market Success (IPMS) of Ethiopian farmers project, International Livestock Research Institute (ILRI)*, Addis Ababa, Ethiopia, Jan 2009.
- [18] B.K.Nayak, Saswati Swapna Dash, "Transient modeling of Z-source chopper with and without ESR used for control of capacitor voltage," *WSEAS Transactions on Circuit and systems*, Vol.13, pp.175-187, 2014.